THE ASTROPHYSICAL JOURNAL, 404:419–424, 1993 February 20

H_0 FOUND BY COMPARING LINEAR DIAMETERS OF M31 WITH SIMILAR FIELD GALAXIES

ALLAN SANDAGE
The Observatories of the Carnegie Institution of Washington, 813 Santa Barbara Street, Pasadena, CA 91101
Received 1992 July 31; accepted 1992 August 26

ABSTRACT

The method of finding a stringent upper limit to H by comparing the known linear size of M101 with similar field galaxies and requiring that M101 not be the largest in a distance-limited sample is extended here to Sab and Sb galaxies using M31 as the calibrator. In agreement with the earlier result using M101, the upper limit using M31 is $H < 85$ km s^{-1} Mpc^{-1}. Because M31 is the nearest Sb spiral, the most probable actual value of H is found by equating the known linear diameter of M31 with the mean of a distance-limited sample of similar galaxies. Data on 60 RSA galaxies that are similar to M31 give the most probable value as

$$H = 45 \pm 12 \text{ km s}^{-1} \text{ Mpc}^{-1}$$

by this method.

Subject headings: cosmology: observations — distance scale — galaxies: fundamental parameters — galaxies: individual (M31) — galaxies: spiral

1. INTRODUCTION

It was shown in a previous paper (Sandage 1993, hereafter Paper I) that if the Hubble constant were as large as 85 km s^{-1} Mpc^{-1}, and if M101 is at a distance of $D = 6.9$ Mpc $[(m - m)_0 = 29.2]$, then M101 would be among the largest several ScI galaxies within the distance limited sample with $v \sim 2500$ km s^{-1} defined by the RSA2 (Sandage & Tammann 1987) catalog. Such a circumstance is unlikely because M101 is the nearest ScI galaxy to us.

A second result was that if the linear diameter of M101 is at its most probable value, equal to the mean of the field galaxy linear diameter distribution, then $H_0 = 43 \pm 11$ km s^{-1} Mpc^{-1}.

The principal criticism of these results is the use of only one calibrator, necessitated by the circumstance that M101 is the only ScI of known distance. The purpose of this paper is to extend the method to field Sab, Sb, and SBb galaxies whose morphologies are similar to M31. As with M101, the known linear diameter of M31 is compared with the linear diameter distribution of similar field galaxies, calculated with various values of H.

Using M31-like galaxies, the result again is that $H < 50$. Cited in Paper I in anticipation of the present paper, this was taken as supporting evidence for the M101 result that a stringent upper limit to H is $\sim$85, unless, now, the doubly unlikely proposition is true that M101 and M31 are both abnormally large for their class within the same distance-limited volume. Details of evidence using M31 are given here.

A caveat is needed. This is not a precise way to H_0; there are too few calibrators, and the intrinsic dispersion at σ log $D \sim 0.10$ (or $\sigma M \sim 0.5$ mag) is large compared, for example, to the σM(max) of Type I supernovae, which is smaller by at least a factor of 2 (Sandage & Tammann 1990; Tammann & Leibundgut 1990). Neither van der Kruit (1986) who first used the method, nor Tammann (1993), nor the discussion of Paper I claimed such. The importance of the method (Humason, Mayall, & Sandage 1956, Appendix C) is its power in setting a stringent upper limit to H. The result is also useful in the present climate of review articles (e.g., Jacoby et al. 1992; van den Bergh 1993), where the impression is given that values of $H < 50$ are highly unlikely. Our claim from the method is in fact that the value of the Hubble constant is more likely to be $H < 50$ than not.

The reason for discussing statistical methods such as this is to make less startling the much more precise determination, in principle, that $H_0 = 45 \pm 11$ km s^{-1} Mpc^{-1} using the method through SN Ia based on Cepheids in IC 4182 (Sandage et al. 1993) and the new methods based on the Sunyaev-Zel'dovich effect (see Birkinshaw, Hughes, & Arnauld 1991), and the time delay in gravitational lenses (Rhee 1991; Press, Rybicki, & Hewitt 1992), both of which give H_0 near 40 ± 10.

2. ANGULAR AND LINEAR DIAMETER DATA FOR M31 LOOK-ALIKES

As in Paper I, the new survey material comprising the Carnegie Atlas of Bright Galaxies (Sandage & Bedke 1993) was inspected to identify all RSA galaxies that have similar morphologies to M31. Strict identity with the SbI–II morphology of M31 was not demanded (no two galaxies are identical). Rather, galaxies of types Sab, Sb, and SBb with a general similarity to M31 were separated from the RSA binning lists and used for this analysis. The data are listed in Tables 1–3.

The morphological type listed in the RSA2, or as modified for the Carnegie Atlas of Bright Galaxies, is in column (2) of each table. The redshift, corrected to the centroid of the Local Group as listed in RSA2, is in column (3). The log of the isophotal angular diameters to an isophote of 25 B-magnitudes per arcsec^2 and reduced to face on, in units of 6″, as listed in the second and third Reference Catalogs (de Vaucouleurs, de Vaucouleurs, & Corwin 1976, hereafter RC2; de Vaucouleurs et al. 1991, hereafter RC3), are in columns (5) and (6). The log linear diameter (in pc) on the angular diameter system of the RC2 and based on redshift distances using column (3) and $H =$ 50 km s^{-1} Mpc^{-1}, is in column (7). The absolute "total" B-magnitudes, based on the $B_T^{0,i}$ apparent magnitude in the RSA and the redshift distance, are in column (8).

As discussed in Paper I, the isophotal diameter system of the RC3, corrected to face-on, differs fundamentally from that of

TABLE 1

REDSHIFTS, DIAMETERS, AND MAGNITUDES FOR Sab GALAXIES SIMILAR TO M31

Name (1)	Type (2)	v_0 (km s^{-1}) (RSA) (3)	log v_0 (4)	log $\theta(0)$ (RC2) (0.′1) (5)	log $\theta(0)$ (RC3) (0.′1) (6)	log $D(0)$ (RC2) pc(H50) (7)	$-M^{0,i}_{B(T)}$ (RSA) (H50) (8)
NGC 488	Sab(rs) I	2442	3.388	1.69	1.73	4.84	22.86
NGC 1398	SBab(r) I	1471	3.168	1.80	1.85	4.73	22.30
NGC 2196	Sab(s) I	2184	3.339	1.42	1.49	4.52	21.95
NGC 2460	Sab(s)	1593	3.202	1.44	1.41	4.40	20.62
NGC 2985	Sab(s)	1451	3.162	1.61	1.66	4.53	21.74
NGC 3329	Sab	2102	3.323	1.27	1.26	4.35	20.92
NGC 4569V	Sab(s) I–II	(−373)	3.058V	1.90	1.99	4.72	22.31V
NGC 4579V	Sab(s) II	(1687)	3.058V	1.71	1.78	4.53	21.69V
NGC 4699	Sab or Sa	1309	3.117	1.53	1.59	4.41	22.24
NGC 5037	Sab(s)	1679	3.225	1.29	1.36	4.28	20.73
NGC 7126	Sab(s) I	2888	3.461	1.29	1.46	4.51	21.61
NGC 7177	Sab(r) II.2	1419	3.152	1.48	1.51	4.39	21.10
NGC 7716	Sab(r) I	2735	3.437	1.34	1.34	4.54	21.26

TABLE 2

REDSHIFTS, DIAMETERS, AND MAGNITUDES FOR Sb GALAXIES SIMILAR TO M31

Name (1)	Type (2)	v_0 (km s^{-1}) (RSA) (3)	log v_0 (4)	log $\theta(0)$ (RC2) (0.′1) (5)	log $\theta(0)$ RC3 (0′1) (6)	log $D(0)$ (RC2) pc(H50) (7)	$-M^{0,i}_{B(T)}$ (RSA) (H50) (8)
NGC 224	Sb I–II	...	...	3.15	3.31	4.46	21.49
NGC 615	Sb(r) I–II	1971	3.295	1.52	1.56	4.58	21.59
NGC 1288	Sb(r) I–II	4461	3.649	1.36	1.36	4.77	22.42
NGC 1325	Sb(s) II	1574	3.197	1.56	1.68	4.52	21.15
NGC 1425	Sb(r) II	1440	3.158	1.66	1.76	4.58	21.53
NGC 1515	Sb(s) II	959	2.982	1.59	1.72	4.33	20.76
NGC 2551	Sb(r) I–II	2484	3.395	1.24	1.22	4.40	21.17
NGC 2613	Sb(s) (II)	1446	3.160	1.74	1.90	4.66	22.71
NGC 2683	Sb (on edge)	399	2.601	1.84	1.98	4.20	20.17
NGC 2841	Sb	714	2.854	1.83	1.91	4.44	21.53
NGC 2889	Sb(r) II	3194	3.504	1.30	1.35	4.56	22.19
NGC 3031	Sb(r) I–II	...	...	2.35	2.44	4.33	20.55
NGC 3038	Sb(s) II	2412	3.382	1.37	1.45	4.51	21.44
NGC 3147	Sb(s) I–II	2899	3.462	1.59	1.59	4.81	22.94
NGC 3169	Sb(r) I–II (tides)	1067	3.028	1.64	1.64	4.43	21.09
NGC 3223	Sb(s) I–II	2619	3.418	1.56	1.66	4.74	22.69
NGC 3241	Sb(r) II	2584	3.412	1.15	1.38	4.32	20.80
NGC 3642	Sb(r) I	1733	3.239	1.74	1.73	4.74	21.69
NGC 3675	Sb(r) II	792	2.899	1.71	1.77	4.37	20.88
NGC 3717	Sb(s)	1443	3.159	1.62	1.80	4.54	21.57
NGC 4216V	Sb(s)	(−8)	(3.058)V	1.78	1.91	4.60	21.94V
NGC 4258	Sb(s) II	520	2.716	2.18	2.27	4.66	22.05
NGC 4814	Sb(s) I	2650	3.423	1.49	1.49	4.67	21.41
NGC 5005	Sb(s) II	1042	3.018	1.66	1.76	4.44	21.78
NGC 5134	Sb(s) (II–III)	1027	3.012	1.39	1.47	4.16	19.96
NGC 5150	Sb(r) I–II	4127	3.616	1.16	1.13	4.54	21.86
NGC 5533	Sb(s) I	3903	3.591	1.47	1.49	4.82	22.48
NGC 5878	Sb(s) I.2	1974	3.295	1.47	1.59	4.53	21.63
NGC 5879	Sb(s) II	929	2.968	1.54	1.62	4.27	20.24
NGC 6384	Sb(r) I.2	1735	3.239	1.75	1.83	4.75	22.28
NGC 6753	Sb(r) I	3001	3.477	1.39	1.41	4.63	22.64
NGC 6887	Sb(s) I–II	2938	3.468	1.52	1.55	4.75	22.42
NGC 6943	Sb(rs) II	2947	3.469	1.54	1.62	4.77	22.61
NGC 7083	Sb(s) I–II	2951	3.470	1.61	1.59	4.84	22.81
NGC 7205	Sb(r) II.8	1379	3.140	1.56	1.61	4.46	21.48
NGC 7217	Sb(r) II–III	1234	3.091	1.55	1.63	4.40	21.66
NGC 7331	Sb(rs) I–II	1114	3.047	1.93	2.06	4.74	22.60
NGC 7782	Sb(s) I–II	5584	3.747	1.32	1.40	4.83	22.88

TABLE 3

REDSHIFTS, DIAMETERS, AND MAGNITUDES FOR SBb GALAXIES SIMILAR TO M31

Name (1)	Type (2)		v_0 (3)	log v_0 (4)	log $\theta(0)$ (RC2) (0.'1) (5)	log $\theta(0)$ (RC3) (0.'1) (6)	log $D(0)$ (RC2) pc(H50) (7)	$-M^{0,i}_{B(T)}$ (RSA) H50 (8)
NGC 613	SBb(rs)	II	1534	3.186	1.74	1.74	4.69	22.24
NGC 986	SBb(rs)	I–II	2006	3.302	1.54	1.59	4.60	21.81
NGC 1433	SBb(s)	I–II	923	2.965	1.82	1.81	4.55	21.15
NGC 1832	SBb(r)	I	1855	3.268	1.40	1.43	4.43	21.53
NGC 3351	SBb(r)	II	641	2.807	1.84	1.88	4.41	20.66
NGC 3504	Sb(s)/SBb(s)	I–II	1480	3.170	1.41	1.43	4.34	21.11
NGC 3681	SBb(r)	I–II	1135	3.055	1.40	1.49	4.22	19.84
NGC 4394V.....	SBb(sr)	I–II	(853)V	(3.058)V	1.59	1.57	4.41	20.42V
NGC 4548V.....	SBb(rs)	I–II	(366)V	(3.058)V	1.71	1.74	4.53	21.27V
NGC 4725	Sb/SBb(r)	II	1167	3.067	2.01	2.03	4.84	22.47
NGC 5985	SBb(r)	I	2694	3.430	1.69	1.74	4.88	21.65

the RC2. In the reductions for the RC3, spiral disks were assumed to be opaque. The correction to face on diameters in the RC2, like those in the RSA, adopted the less extreme Holmberg (1958) precepts for disk absorption. The RC3 face-on isophotal diameters differ systematically with those in the RC2 depending on the inclination of particular galaxies. The effect is seen by comparing columns (5) and (6) in each of the three tables. Diameters on the system of the RC3, again with $H = 50$, can be obtained by adding the difference between columns (6) and (5) to column (7).

In the analysis of this paper, we carry both the RC2 and RC3 diameter precepts. The conclusion is the same using either diameter system, and is the same as in Paper I. Unless M31 is among the largest Sb I–II galaxies in a distance-limited sample of Sab and Sb I–II galaxies in the RSA, the long-distance scale is required, meaning that H_0 is small.

3. COMPARISON OF M31 WITH Sab AND Sb FIELD GALAXIES

3.1. *Diameter and Magnitude Data for M31 and M81*

The isophotal angular diameter of M31 listed in the RC2, corrected to face-on orientation, is 141'. Adopting a distance modulus of $(m - M)_0 = 24.2$ gives a linear isophotal diameter of 28.4 kpc, or log $D(0)_{pc} = 4.45$. The RC3 values are 204' and log $D(0)_{pc} = 4.61$, again assuming $(m - M)_0 = 24.2$. If $(m - M)_0 = 24.4$ as advocated by Freedman & Madore (1990), the linear diameter values become larger by a factor of 1.1, giving log $D(0)_{RC2} = 4.49$ and log $D(0)_{RC3} = 4.65$ with a corresponding increase in the value of H derived if $(m - M)_0 = 24.2$.

The apparent magnitude of M31 listed in the RSA2, corrected for Galactic and internal absorption by the precepts of that catalog, is $B^{0,i}_T = 2.71$. The corresponding absolute magnitude is $M^{0,i}_{B(T)} = -21.49$, again using $(m - M)_0 = 24.2$.

The values for M81, used later in Figure 1 are, log $D(0)_{pc} = 4.33$ from the RC2 angular diameter, and log $D(0)_{pc} = 4.42$ from the RC3 angular diameter using $(m - M) = 27.6$. The $B^{0,i}_T$ magnitude corrected for Galactic and internal absorption is 7.01, giving $M^{0,i}_{B(T)} = -20.59$.

3.2. *The Field Galaxy Data*

Figure 1 shows the correlation of linear diameters with absolute magnitude from the data in Tables 1–3 for the field galaxies, calculated assuming $H = 50$ km s^{-1} Mpc^{-1}. Diameters based on RC3 isophotal angular diameters are in the top panel. Diameters based on the data in the RC2 are used in the lower panel. Also plotted are the diameter and absolute magnitude values for M31 and M81 from the last section. These are based on Cepheid distances to these galaxies and are therefore independent of H. With $H = 50$ used for all galaxies except M31 and M81, M31 lies near the mean of the distributions of both the ordinate and abscissa in Figure 1. For different values of H, the ordinate and abscissa values of the field galaxies

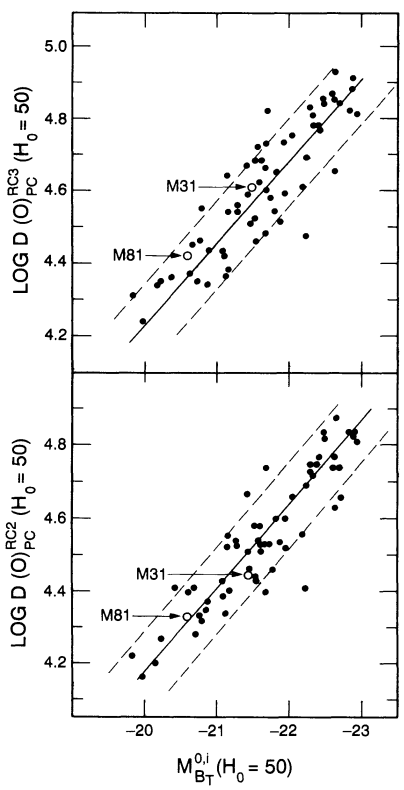

FIG. 1.—(*a*) Correlation of RC3 linear diameters with RSA absolute magnitudes for the complete sample of galaxies in Tables 1–3, calculated with $H = 50$ and RSA v_0 redshifts. Positions of M31 and M81 shown using Cepheid distances of $(m - M)_0 = 24.2$ and 27.6, respectively. The coordinates for M31, using the RC3 angular diameter corrected to face on and the RSA fully corrected apparent magnitude is log $D = 4.61$ and $M^{0,i}_{B(T)} = -21.49$. (*b*) Same as Fig. 1*a* but using RC2 angular diameters. The coordinates for M31 are log $D = 4.45$ and $M^{0,i}_{B(T)} = -21.49$. Equation of the ridge line is log $D = -0.23M^{0,i}_{B(T)} = -0.42$. Envelope lines are drawn by eye. If $(m - M)_0 = 24.4$ for M31, the M31 ordinate values in both panels are increased by 0.04 and the abscissa value is made brighter by 0.2 mag.

change relative to the M31 and M81 points. This is used as the main part of the argument later in Figures 5 and 6 to find what value of H is required to make M31 average rather than supergiant size.

The conclusion reached in this paper is already evident from Figure 1. If H were as high as 85, M31 would be near the top of the diagram rather than near the middle of both the ordinate and the abscissa distributions. This is highly unlikely because M31 is the nearest Sb galaxy to us.

To assess quantitatively the limits on H that can be put with this method we need to make a more detailed analysis. The Malmquist bias must be removed. It enters with its full strength because the sample in Tables 1–3 is from the flux-limited RSA catalog rather than being distance limited. The method to define a distance-limited sample as a subset of the data is the same as used in Paper I, based on an earlier analysis using limit lines in the log D, log v_0 diagram, equivalent to the M_T, log v_0 bias diagram used in Sandage (1988a, b, hereafter S88a, b).

The linear diameters (based on $H = 50$) from Tables 1–3 are plotted versus log v_0 in Figure 2 using RC2 diameters. The top panel shows the correlation of diameters with redshift. The apparent systematic increase of log D with increasing redshift is due to the Malmquist bias caused by the selection effect that small diameter galaxies are progressively denied entry into the sample at progressively larger redshifts because of the magnitude limit of the RSA catalog. The proof that this is a selection bias, not due to an increase of H outward as claimed by Tully (1988), has been given elsewhere (S88a, b) by adding a fainter sample. The presence of a selection bias can always be tested in this way. If a supposed systematic effect disappears in the fainter sample at the level where it appears in the brighter sample only to reappear again near the limit of the fainter sample, it is certain that the effect is due to selection bias and is not real. The apparent increase in the mean log D-values in each redshift interval, shown in the top panel of Figure 2, is due to this Malmquist effect, similar in every way to the effect seen in S88a, b and in Paper I.

The effect is illustrated in the bottom panel of Figure 2 where limit lines are shown, based on a Gaussian approximation to distribution of log D-values with $\sigma \log D = 0.10$ (see Paper I). The opening of the curved limit lines outward with increased redshift is due to the increased normalization factor of the assumed Gaussian distribution with increasing volume in each successive redshift interval. The straight solid and dashed limit lines are the limits on log D expected from the RSA effective apparent magnitude limit of $B_T^{0,i} = 12.5$. The solid line is calculated from the ridge line from Figure 1. The dashed line is based on the lower envelope line in the same diagram, calculated as described in Paper I.

Figure 3 shows the similar diagram using RC3 angular diameters, converted to linear diameters using redshift distances with $H = 50$. (The data in Tables 1–3 have not been corrected for Virgo "infall" as in Paper I. Numerical experiments with and without this correction show that the effect on the statistical sample as a whole can be neglected in the mean

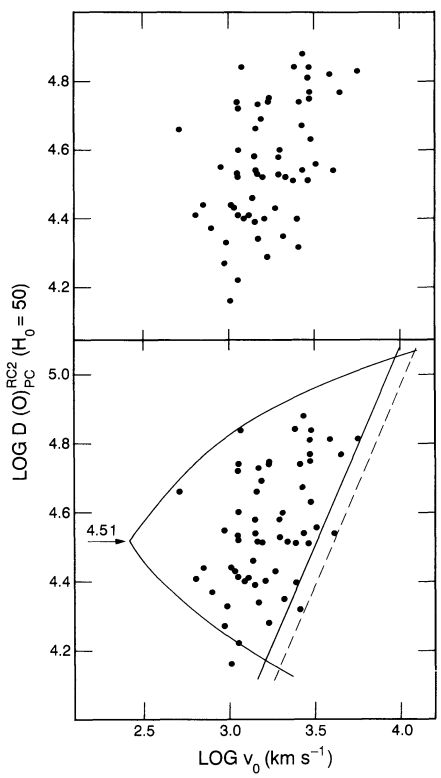

FIG. 2.—(*a*) Correlation of RC2 linear diameters for the complete sample in Tables 1–3 with log redshift corrected to the centroid of the Local Group. The apparent increase of diameter with increasing redshift is caused by Malmquist sample bias, as shown in the bottom panel. The linear diameters are calculated assuming $H = 50$. (*b*) Same as Fig. 2*a* but with limit lines superposed. The curved lines are due to the increased volume normalization factor with increasing redshift. The straight lines are due to the flux limitation in the RSA catalog. The solid line is transposed from the ridge line of Fig. 1*b*. The dashed line is from the lower envelope line in the same diagram. The arrow identifies the calculated mean log D for the sample, fully corrected for Malmquist bias.

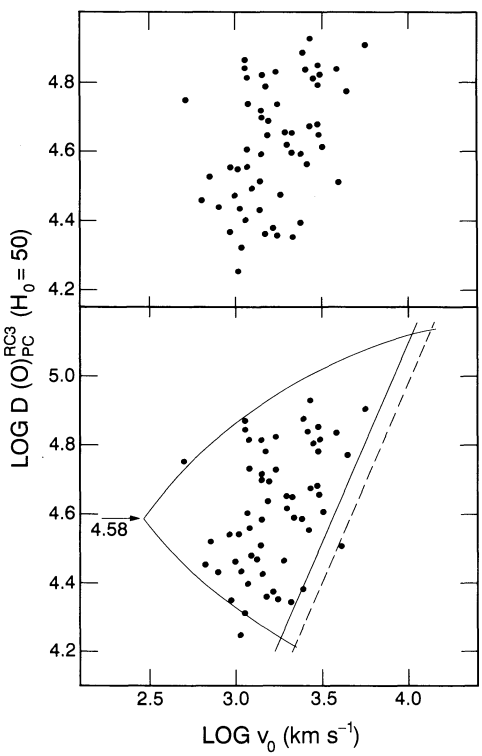

FIG. 3.—Same as Fig. 2 but using RC3 diameters

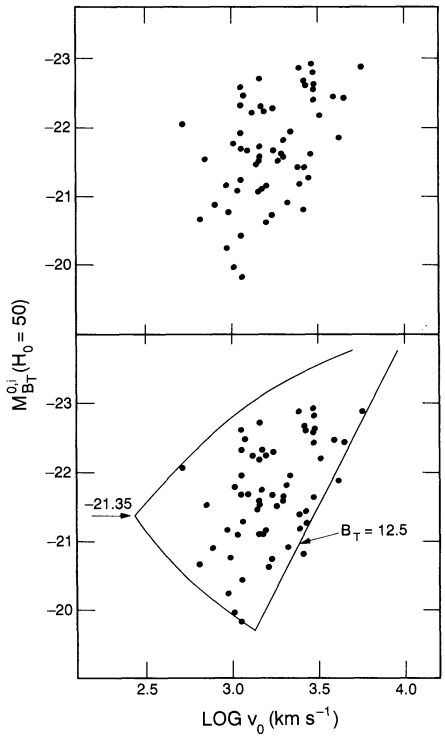

FIG. 4.—Same as Figs. 2 and 3 but using RSA absolute magnitudes

at the level needed for the argument made in this paper and in Paper I.)

A different representation, nearly equivalent because of the tight correlation in Figure 1, can be made using the absolute magnitude, redshift bias diagram as was done earlier (S88a). The apparent correlation showing brighter average absolute magnitudes at larger redshifts, is shown in Figure 4*a* using the data from columns (4) and (8) of each of the Tables 1–3. Again, the apparent correlation is due to the Malmquist selection bias, proved by showing the limit lines in the bottom panel. These lines are based on $\sigma M = 0.5$ mag, and the effective RSA limiting apparent magnitude of $B_T = 12.5$.

As evident from Figures 2–4, the subset of the sample in Tables 1–3 that is distance limited is contained within the limit lines in each figure, as bounded by the curved volume normalization lines and the straight limit lines at a redshift where they intersect the bottom curved normalization limit line. This occurs near log $v \sim 3.3$ in each diagram corresponding to a distance of 2000 km s^{-1}. Such a distance-limited sample is discussed later from Figures 5 and 6, set out there.

3.3. *Setting the Apex Positions in Figures 2–4*

The apex position of the envelope lines along the ordinate of Figures 2–4 define the mean position of the distance-limited subsample in Tables 1–3. In the first application of the method with a different data set (S88a, b), the apex position was determined by eye using vertical and horizontal sliding fits until most of the data were accommodated. In Paper I (§ 5.2), the vertical position was determined by integrating assumed Gaussian distributions for log D in separate redshift intervals, progressively truncating each distribution by the straight limit lines defined by the flux limitation of the RSA, similar to those in Figures 2–4. We apply the same procedure here. Details of the method given in Paper I are not repeated here.

Consider first the data using RC2 diameters in Figure 2. The mean of the log D data in the distance-limited subset of the sample defined for log $v < 3.20$, is $\langle \log D \rangle = 4.45$. Between log v of 3.2 and 3.4, the mean is 4.53, from which we must subtract 0.02 for the calculated Malmquist bias following equation (3) of Paper I. In the largest redshift interval of log $v > 3.4$, the mean of the raw data is $\langle \log D \rangle = 4.62$ to which a calculated bias correction of -0.12 is applied. The mean of the values, corrected for bias, is $\langle \log D \rangle = 4.51$, shown by the arrow in Figure 2. The formal error in this value is $\Delta \log D = 0.05$, agreeing with the visual estimate from Figure 2 of how much we may shift the curved limit lines vertically without compromising the data.

The results of the same calculation using RC3 diameters (found from Tables 2–4 by adding the difference between cols. [6] and [5] to col. [7]), is shown by the arrow in Figure 3*b* at $\langle \log D \rangle = 4.58$. The same type of calculation using the absolute magnitudes in column (8) of Tables 1–3, as in S88a, gives $\langle M^{0,i}_{B(T)} \rangle = -21.35$ using the RSA magnitudes based on the precepts in that catalog for fully corrected magnitudes.

4. THE HUBBLE CONSTANT

Combining the adopted data for M31 from § 3.1 based on $(m - M)_0 = 24.2$ with the apex values for $\langle \log D \rangle$ in Figures 2–4, and imposing the requirement that the known diameter of M31 be equal to these mean values (calculated with the appropriate H value to make it so), gives the following values for the Hubble constant. Using RC2 diameters in Figure 2 with the apex value of $\langle \log D \rangle = 4.51$ gives $H = 57 \pm 16$ km s^{-1} Mpc^{-1}, found by using $(\log D)_{RC2} = 4.45$ for M31, based on $(m - M)_0 = 24.2$. The quoted formal error assumes that the uncertainty in the apex level in Figure 1 is $\Delta \log D = 0.05$ and that the dispersion in the distribution of linear diameters is 0.10. This gives a total uncertainty to be $\Delta \log D = 0.11$, or 29% in H_0.

On the other hand, if $(m - M)_0 = 24.4$ for M31 (Freedman & Madore 1990), the value using RC2 diameters becomes

$$H = 51 \pm 15 \text{ km s}^{-1} \text{ Mpc}^{-1} . \quad (1)$$

Using RC3 diameters and the apex value of $\langle \log D \rangle_{RC3} = 4.58$ from Figure 4, combined with $\log D_{RC3} = 4.61$ for M31 from the RC3, again with $(m - M)_0 = 24.2$, gives $H = 47 \pm 14$ km s^{-1} Mpc^{-1} if the diameter of M31 is equal to the mean diameter of the field galaxies. On the other hand, if $(m - M)_0 = 24.4$ for M31, the RC3 diameter data require

$$H = 42 \pm 12 \text{ km s}^{-1} \text{ Mpc}^{-1} . \quad (2)$$

Finally, from Figure 4, using $\langle M^{0,i}_{B(T)} = -21.49$, based on $B^{0,i}_T = 2.71$ from the RSA and $(m - M)_0 = 24.2$, then $H_0 = 47 \pm 14$. The quoted error is based on $\sigma M_T = 0.5$ mag combined with an assumed uncertainty of the apex position in Figure 4 of 0.25 mag. On the other hand, again if $(m - M)_0 = 24.4$, then $M^{0,i}_{B(T)} = -21.69$ for M31, giving

$$H = 42 \pm 12 \text{ km s}^{-1} \text{ Mpc}^{-1} , \quad (3)$$

using $\langle M_{B(T)} \rangle = -21.35$ for the field galaxies from Figure 4.

As discussed in Paper I, the correction of this local value to the global value, H_0, is known to be small (Sandage, Tammann, & Hardy 1972; Sandage & Tamman 1975, 1982, 1990; Tammann & Sandage 1985; Jerjen & Tammann 1993). Hence the conclusion from equations (1)–(3) is that the most

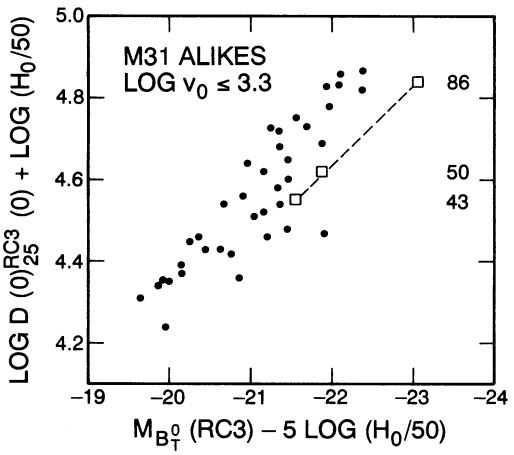

FIG. 5.—Same as Fig. 1 but using RC3 fully corrected magnitudes and the subsample from Tables 1–3 that is distance limited. The position of M31 relative to the field galaxies for three values of H is shown, based on $(m - M)_0 = 24.2$, log D(M31) = 4.61, and $M^0_{B(T)} = -21.86$. As H is varied, the position of M31 relative to the field galaxies changes.

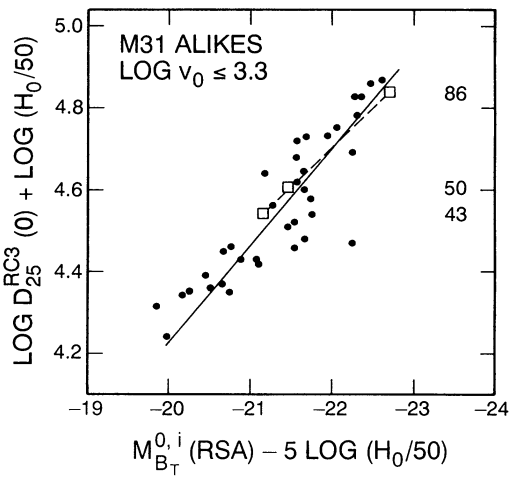

FIG. 6.—Same as Fig. 5 but using RSA fully corrected magnitudes. The adopted absolute magnitude of M31 on this system is $M^{0,i}_{B(T)} = -21.49$. If $(m - M)_0 = 24.4$ for M31, the ordinates of the M31 points increase by 0.04 and the abscissa values become brighter by 0.2 mag.

probable value for H is close to 45 from the Sab and Sb I–II field galaxy data and, therefore, that H_0 is closer to 50 than to 85.[1]

5. UPPER LIMIT TO H

As stated in the introduction, the method to H discussed here clearly is not precise because spiral galaxies, even if restricted in luminosity class, have wide dispersions in both M_T and log D, the two being related by $\sigma\ M_T \sim 5\ \sigma$ log D. Nevertheless, the method is precise enough to show, as in Paper I (Figs. 6 and 7), that H as high as 85 is unlikely. We repeat that demonstration here by using M31.

Figures 2–4 show that the distance-limited subsample in Tables 1–3 is defined by galaxies with log v smaller than about 3.3. This is the approximate redshift where the straight limit lines met the lower limit curved boundary line. All galaxies in Tables 1–3 with this redshift restriction are plotted in Figure 5 using RC3 diameters and $M^0_{B(T)}$ magnitudes also from the RC3. The diagram is similar to Figure 1*a*, except that only the distance-limited sample is used, and RC3 rather than RSA apparent magnitudes are used.

The position of M31 relative to the field galaxies are shown for different H-values using the data from § 3.1 with $(m - M)_0 = 24.2$. The point of the diagram is to show that, as in Paper 1, M31 lies near the mean of the field galaxy distribution in both diameter and absolute magnitude if $H = 43$. At twice that value, $H = 86$, M31 would be among the largest and brightest of the sample, as in Paper 1 using M101.

Figure 6 requires the same conclusion, again using RC3 diameters but now $M^{0,i}_{B(T)}$ magnitudes from the RSA.

6. CONCLUSIONS

Two conclusions follow from Figures 2–6. (1) The most probable value of the Hubble constant, based on linear diameters and absolute magnitudes of RSA field galaxies similar to M31 in a distance-limited sample, is H 45 ± 12 km s^{-1} Mpc^{-1}, found by combining results using RC2 and RC3 diameters from equations (1) and (2) with equation (3) using magnitudes, using $(m - M)_0 = 24.4$ for M31. (2) If $H \sim 85$, then the improbable situation would exist that both M31 and M101 would be among the largest spirals of their class within the distance-limited samples of the RSA, despite their both being the closest galaxies of their types.

[1] Had we attempted to use only the five Virgo Cluster spirals in Tables 1–3, following the method of van der Kruit (1986), setting aside the discussion of Teerikorpi et al. (1992) on the danger of assuming that any subset of spirals in the region of the cluster defines the distance to the Virgo Cluster core, the results, uncertain as they are, would be as follows. Adopting $(m - M)_0 = 24.4$ for M31 from Freedman & Madore (1990), and equating its linear diameter to the mean of the Virgo Cluster sample gives $H = 58$ using RC2 diameters, and $H = 46$ using RC3 diameters for both M31 and the five Virgo Cluster listings in the tables.

REFERENCES

Birkinshaw, M., Hughes, J. P., & Arnauld, K. A. 1991, ApJ, 379, 466
de Vaucouleurs, G., de Vaucouleurs, A., & Corwin, H. G. 1976, Second Reference Catalog of Bright Galaxies (Austin: Univ. Texas Press) (RC2)
de Vaucouleurs, G., de Vaucouleurs, A., Corwin, H., Buta, R. J., Paturel, A., & Fouque', P. 1991, Third Reference Catalog of Bright Galaxies (Berlin: Springer) (RC3)
Freedman, W. L., & Madore, B. F. 1990, ApJ, 365, 186
Holmberg, E. 1950, Medd. Lunds Astron. Obs. 128
Humason, M. L., Mayall, N. U., & Sandage, A. 1956, AJ, 61, 97
Jacoby, G., et al. 1992, PASP, 104, 599
Jerjen, H., & Tammann, G. A. 1993, A&A, in press
Press, W. H., Rybicki, G. B., & Hewitt, J. N. 1992, ApJ, 385, 404
Rhee, G. 1991, Nature, 350, 211
Sandage, A. 1988a, ApJ, 331, 583
———. 1988b, ApJ, 331, 605
———. 1993, ApJ, 402, 3 (Paper I)
Sandage, A., & Bedke, J. 1993, Carnegie Atlas of Bright Galaxies (Washington, DC: Carnegie Inst. of Washington)
Sandage, A., Saha, A., Tammann, G. A., Panagia, N., & Macchetto, F. 1993, ApJ, 401, L7
Sandage, A., & Tammann, G. A. 1975, ApJ, 196, 313
———. 1982, ApJ, 256, 339
———. 1987, A Revised Shapley-Ames Catalog 2d ed. (Washington, DC: Carnegie Inst. of Washington)
———. 1990, ApJ, 365, 1
Sandage, A., Tammann, G. A., & Hardy, E. 1972, ApJ, 172, 253
Tammann, G. A. 1993, Phys. Scripta, in press
Tammann, G. A., & Leibundgut, B. 1990, A&A, 236, 9
Tammann, G. A., & Sandage, A. 1985, ApJ, 294, 81
Teerikorpi, P., Bottinelli, L., Gougenheim, L., & Paturel, G. 1993, in press
Tully, B. 1988, Nature, 334, 209
van den Bergh, S. 1993, PASP, 104, 861
van der Kruit, P. 1986, A&A, 157, 230